

# Computer-based Studies of Diffusion through Stomata of Different Architecture

ANITA ROTH-NEBELSICK\*

*Institute for Geosciences, University of Tübingen, D-72076 Tübingen, Germany*

Received: 9 January 2007 Returned for revision: 19 February 2007 Accepted: 9 March 2007 Published electronically: 4 May 2007

• **Background and Aims** The influence of stomatal architecture on stomatal conductance and on the developing concentration gradient was explored quantitatively by comparing diffusion rates of water vapour and CO<sub>2</sub> occurring in a set of three-dimensional stoma models. The influence on diffusion of an internal cuticle, a sunken stoma, a partially closed stoma and of substomatal chambers of two different sizes was considered.

• **Methods** The study was performed by using a commercial computer program based on the Finite Element Method which allows for the simulation of diffusion in three dimensions. By using this method, diffusion was generated by prescribed gas concentrations at the boundaries of the substomatal chamber and outside of the leaf. The program calculates the distribution of gas concentrations over the entire model space.

• **Key Results** Locating the stomatal pore at the bottom of a stomatal antechamber with a depth of 20 µm decreased the conductance significantly (at roughly about 30 %). The humidity directly above the stomatal pore is significantly higher with the stomatal antechamber present. Lining the walls of the substomatal chamber with an internal cuticle which suppresses evaporation had an even stronger effect by reducing the conductance to 60 % of the original value. The study corroborates therefore the results of former studies that water will evaporate preferentially at sites in the immediate vicinity to the stomatal pore if no internal cuticle is present. The conductance decrease affects only water vapour and not CO<sub>2</sub>. Increasing the substomatal chamber increases CO<sub>2</sub> uptake, whereas transpiration increases if an internal cuticle is present.

• **Conclusions** Variation of stomatal structure may, with unchanged pore size and depth, profoundly affect gas exchange and the pathways of liquid water inside the leaf. Equations for calculation of stomatal conductance which are solely based on stomatal density and pore depth and size can significantly overestimate stomatal conductance.

**Key words:** Gas exchange, diffusion, stomata, stomatal conductance, internal cuticle, sunken stomata, stomatal antechamber.

## INTRODUCTION

The diffusive conductance of a leaf is mainly dependent on boundary layer and stomatal conductance (or resistance). There are various approaches for modelling the regulation of stomatal conductance as a response to environmental and physiological factors (e.g. Farquhar and Wong, 1984; Ball *et al.*, 1987; Leuning, 1990; Collatz *et al.*, 1991; Buckley *et al.*, 2003). These models consider the plant control mechanisms of actual pore size. Besides the instantaneous pore size, stomatal conductance is dependent on various structural features, such as stomatal density, pore shape and depth, and the degree of interference between adjacent stomata. Theoretical approaches for calculating stomatal conductance are based on these parameters (Brown and Escombe, 1900; Parlange and Waggoner, 1970; Lushnikov *et al.*, 1994). The size of the substomatal chamber also influences stomatal conductance. It was found for a simple cylindrical model that the rate of water vapour flux decreases until the substomatal chamber reaches the size of a few pore radii (Pickard, 1981). Larger sizes which are usually realized for real stomata can promote CO<sub>2</sub> uptake (Pickard, 1982). By applying the equation of Parlange and Waggoner (1970) to an elongated slit, Van Gardingen *et al.* (1989) achieved very good agreement between calculated and measured conductance for *Avena*

*fatua* after determining the actual stomatal pore sizes by Cryo-SEM.

Stomatal architecture, however, shows a large variability among plants and many features are interpreted as influencing stomatal conductance. For example, sunken stomata, seated at the bottom of a recess termed the stomatal antechamber (Napp-Zinn, 1973) or stomata located in crypts or grooves (housing more than one stoma; Napp-Zinn, 1973) are considered as xeromorphic properties decreasing stomatal conductance (Lösch *et al.*, 1982; Larcher, 2003). Lösch *et al.* (1982) compared the transpiration rates of two shrub species, *Eriobotrya japonica* and *Nerium oleander*. He suggested that the lower conductance of *E. japonica* might be due to the dense hair covering the abaxial leaf surfaces which possibly decreases conductance more effectively than the sunken stomata of *N. oleander*. Another feature which is expected to decrease the conductance are stomatal wax plugs which are especially common in conifers (and which often also have sunken stomata). Brodribb and Hill (1997) reported that stomatal wax plugs decrease leaf conductance significantly. They interpreted wax plugs, however, not as an adaptation to drought, but as a means to prevent the formation of a water film over the stomatal pore during rain or mist (Brodribb and Hill, 1997). On the contrary, Feild *et al.* (1998) found that stomatal plugs of *Drimys winteri* lead to a minor resistance increase of about 8 %.

\* E-mail anita.roth@uni-tuebingen.de

Internal cuticles are also expected to influence stomatal diffusion. Cuticular substances which cover mesophyll cell walls adjacent to intercellular air spaces were found in a number of different species (Scott, 1948; Norris and Bukovac, 1968; Wullschleger and Oosterhuis, 1989; Pesacreta and Hasenstein, 1999). The extent of the internal cuticle differs for different species and is also subject to controversial discussion (Pesacreta and Hasenstein, 1999). The efficiency of an internal cuticle as an evaporative barrier is unclear. It is usually much thinner than the external cuticle, but no conclusion can be drawn from the thickness of the internal cuticle to its capacity to prevent water loss (Pesacreta and Hasenstein, 1999). Since there is evidence that evaporation is strongest close to the stoma if no evaporative barrier exists (Tyree and Yianoulis, 1980; Pickard, 1981; Yianoulis and Tyree, 1984), any decrease of evaporation in the vicinity of the stomatal pore should influence diffusion. Cuticle-free areas on the inner walls of guard cells of several tree species were interpreted as sites of strong evaporation which were involved in the humidity response of the stomata (Appleby and Davies, 1983).

The model approaches mentioned so far are based on different simplifications of the stomatal structure. They describe diffusion through channels with elliptic or circular cross-section (Parlange and Waggoner, 1970; Lushnikov *et al.*, 1994) or diffusion through circular pores located above a substomatal chamber which is hemispherical or cylindrical (Tyree and Yianoulis, 1980; Pickard, 1981, 1982; Yianoulis and Tyree, 1984). In all these cases, the pore aperture was located at the same level as the epidermis. In some models, a stomatal channel was not integrated. If the models included a substomatal chamber, then evaporation was allowed at the entire chamber wall. One model variation of Pickard (1981) included an internal cuticle leading to a significant reduction of conductance. It was, however, located at the ceiling around the stomatal pore which lacked a stomatal channel. The simplifications depended on the aspects considered and were necessary if a mathematical-analytical approach was applied. A numerical study which considered gaseous exchange through a stoma whose geometry is based on *Pinus sylvestris* and which included an antechamber and a substomatal cavity (both cylindric) was performed by Vesala *et al.* (1995, 1996). They found that gas exchange is insensitive to moderate variations of size and shape of the sub-stomatal cavity.

In this contribution, diffusion in different stomata with a stomatal channel located above a substomatal chamber is simulated in order to explore the quantitative influence of the position of the pore, the presence of an internal cuticle and the size of the substomatal chamber on conductance. This is accomplished by applying a computer simulation approach based on the Finite Element (FE) method. This method allows for the consideration of physical processes occurring in complex structures which are represented by a mesh consisting of defined geometrical entities, such as triangular or quadrilateral elements. Diffusion of both water vapour and CO<sub>2</sub> is considered for six different stoma models. The stoma models differ with

respect to location of the pore (sunken versus non-sunken), the presence of an internal cuticle which restricts evaporation inside the substomatal chamber and the size of the chamber. The modelling approach focuses on diffusion through a single stoma only, i.e. the boundary layer above the leaf or interference between adjacent stomata are not considered.

## MATERIALS AND METHODS

### Model technique

The process of diffusion, according to Fick's law, reads for three dimensions as [ $J$  = diffusional flux,  $D$  = diffusion coefficient,  $C$  = concentration, grad = differential operator (M/Mx, M/My, M/Mz)]:

$$J = -D \text{ grad } C \quad (1)$$

This differential equation can be solved only for simple geometric problems, such as circular or elliptic pores or capillaries. It is, however, possible to consider diffusion in more complex three-dimensional structures by using numerical methods, such as the FE method. Due to availability of high amounts of computer resources nowadays it is possible to treat three-dimensional FE models with a high spatial resolution on common PCs. In this contribution, the commercial FE-based program FIDAP 8.7 (Fluent Inc., Lebanon, USA) was applied. FIDAP is a CFD (Computational Fluid Dynamics) program which also includes a diffusion module.

FE is a numerical approach to the solution of differential equations (Zienkiewicz and Taylor, 1989). By using this method, the considered continuum (the continuous space) is divided into a number of elements with prescribed geometry, usually triangular or quadrilateral elements, which are interconnected at their nodes. The aim is to transform the differential equations describing the continuum into a system of algebraic equations describing the behaviour of the interconnected discrete elements. The system of algebraic equations is then solved by iterative numeric procedures for the population of elements which compose the considered geometry. Each change in geometry requires the construction of a new mesh, whereas changes in non-geometrical model components (such as the diffusion coefficient) are simply achieved by changing the input parameters. The results are calculated for the steady state.

The procedure of creating and running a model consists of several steps. Firstly, the desired mesh is created by using an appropriate model generator program. Then the physical problem together with its solution routines is defined. After running the solution module of the program, a data file with the results at each element node is available. Successful application of FE requires the construction of a grid or mesh which shows a certain minimum density of elements. This minimum density is obtained by subsequently increasing the number of elements until the calculated results do not change significantly.

### The FE models

Each of the stomatal variations considered represents an FE model. The six different models are summarized in Table 1. The basic three-dimensional geometry BASIC model is depicted in Fig. 1. It consists of a stomatal channel which connects leaf surface and substomatal chamber. The stomatal pore size shows a broad range of variation in plants. In a survey concerning stomatal dimensions by Napp-Zinn (1973), a range of 7.5–36.5  $\mu\text{m}$  is given as a characteristic magnitude of common pore lengths. Various examples of taxa with stomatal pore lengths of this size can also be found in Metcalfe and Chalk (1979). Much larger sizes occur but these represent the extreme values. A standard pore size of  $12 \times 10 \mu\text{m} = 120 \mu\text{m}^2$  was chosen for the model, because this value appears to lie within the typical range found for mesophytic plants. All models show this pore size, with the exception of one model (CLOS). Here the pore is partially closed with a pore area of  $48 \mu\text{m}^2$  ( $12 \times 4 \mu\text{m}$ ) in order to test the correctness of the model. A value of  $10 \mu\text{m}$  was chosen for the length of the channel (= stomatal pore depth) for all models. This value appears to lie within the typical range for channel depths (Metcalfe and Chalk, 1979). SUNK represents a model of a sunken stoma. Here, the stomatal pore is seated at the bottom of a stomatal antechamber. The antechamber is  $20 \mu\text{m}$  deep with an area of  $12 \times 30 \mu\text{m} = 360 \mu\text{m}^2$ . A cross-sectional view (perpendicular to the pore) of the different models is provided in Fig. 2 which also shows the evaporative sites of the models (see below).

The substomatal chamber has a funnel-shaped geometry (with the stem of the funnel representing the lower side of guard cells) with a length (dimension perpendicular to the pore) of  $25 \mu\text{m}$ . The width (dimension perpendicular to the long axis of the stoma) amounts to  $30 \mu\text{m}$  and the depth (dimension parallel to the long axis of the stoma) amounts to  $12 \mu\text{m}$  (see Figs 1 and 2). Size and shape of the substomatal chamber differs among plant taxa. The actual chamber size and shape was chosen, because only simple hemispherical or cylindrical shapes were considered so far and, according to the results of Pickard (1981, 1982), the chamber size shows no significant effect on water vapour diffusion once a chamber length and width of about twice the pore width is achieved. Two models, CHAM and CHAINT, are equipped with a larger substomatal chamber, and are also

depicted in Fig. 1. In these models, the depth of the substomatal chamber amounts to  $30 \mu\text{m}$ .

Additionally, the evaporative sites were varied. Figure 2 shows the evaporative and non-evaporative sites (= covered by an internal cuticle). In the BASIC, CLOS, SUNK and CHAM models, only the stomatal channel is covered by an internal cuticle completely suppressing evaporation. All other internal parts of the model are sources of water vapour of a defined concentration (for the assignments of water vapour concentrations see below). In the INTERN and CHAINT models, the internal cuticle covers the lateral walls of the substomatal chamber (see Fig. 2).

### Physical parameters

For the model calculations, a temperature of  $20^\circ\text{C}$  is chosen. No temperature gradient is included and the diffusional constants for water vapour ( $2.42 \cdot 10^{-5} \text{ m}^2 \text{ s}^{-1}$ ) and  $\text{CO}_2$  ( $1.5 \cdot 10^{-5} \text{ m}^2 \text{ s}^{-1}$ ) at  $20^\circ\text{C}$  were applied. The model does not take into account temperature gradients which alter the absolute concentrations of water vapour for a certain relative humidity. Results obtained by model calculations performed by Yianoulis and Tyree (1984) indicated that evaporation at the leaf interior leads to cooling effects which decrease the temperature of the evaporating sites to about  $0.1$ – $0.4^\circ\text{C}$ . These alter the concentration gradients slightly but do not change the overall diffusion pattern. The external concentration of water vapour amounts to 50 % relative humidity. A relative humidity of 99 % is assigned to the evaporative sites (Farquhar and Raschke, 1978). This value is also assigned to the bottom of the substomatal chamber for all models.

The external  $\text{CO}_2$  concentration is defined to amount to 360 ppm. The  $\text{CO}_2$  sink created by photosynthesis is represented by a  $\text{CO}_2$  concentration at the bottom of the substomatal chamber, defined as 70 % of the external value (=250 ppm). Only the bottom of the substomatal chamber is equipped with this  $\text{CO}_2$  sink, because the assimilating tissues can be far away from stomata (e.g. the palisade parenchyma in the case of hypostomatous leaves). The model includes only the substomatal chamber close to the stomatal channel and not its continuations into the intercellular air spaces between the assimilating cells.

The ratio of 0.7 between internal and external  $\text{CO}_2$  was chosen as sink strength because values from 0.6–0.8 are commonly observed for many species under optimum

TABLE 1. Summary of the different models

|                                   | BASIC | INTERN | CLOS | SUNK | CHAM  | CHAINT |
|-----------------------------------|-------|--------|------|------|-------|--------|
| Pore area ( $\mu\text{m}^2$ )     | 120   | 120    | 48   | 120  | 120   | 120    |
| Internal cuticle                  | No    | Yes    | No   | No   | No    | Yes    |
| Chamber length ( $\mu\text{m}$ )* | 12    | 12     | 12   | 12   | 32    | 32     |
| Sunken stoma                      | No    | No     | No   | Yes  | No    | No     |
| Transpiration (%)                 | 100   | 59.5   | 46.1 | 71.3 | 98.6  | 74.5   |
| $\text{CO}_2$ influx (%)          | 100   | 100    | 52.9 | 75.8 | 124.2 | 124.2  |

The features which were varied are provided for each model.

Also shown are the differences in the fluxes of water vapour and  $\text{CO}_2$ , expressed as percentage values of the flux rates of the BASIC model.

\*Chamber dimension parallel to the long axis of the stomatal pore.

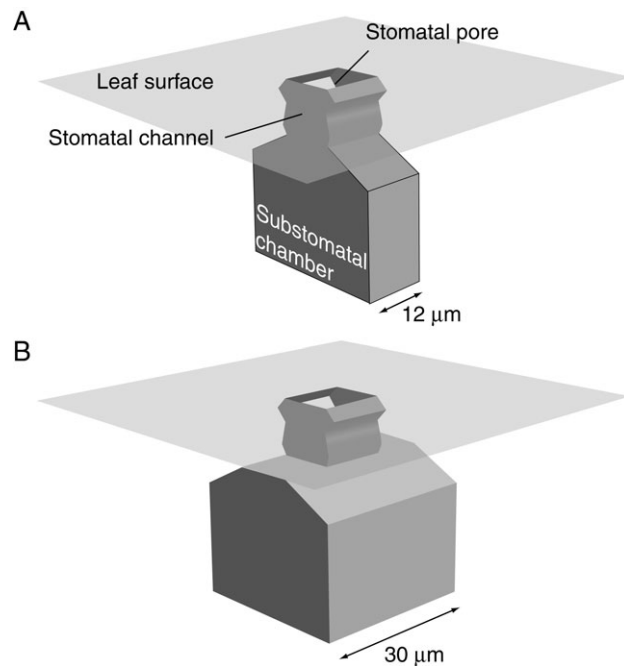


FIG. 1. Basic geometry of the three-dimensional model with a smaller (A) and a larger (B) substomatal chamber. It includes a stomatal porous which is connected to the chamber by a stomatal channel. The model also comprises an air layer adjacent to the leaf surface which has a thickness of  $35\ \mu\text{m}$ . The dimension of the pore is  $10 \times 12\ \mu\text{m}$ , the depth of the channel amounts to  $10\ \mu\text{m}$ . The smaller substomatal chamber has a length of  $12\ \mu\text{m}$  and the length of the larger chamber amounts to  $30\ \mu\text{m}$ . For the other model dimensions see text and the cross-sectional representations in Fig. 2.

conditions (e.g. Franks and Farquhar, 1999). The detailed patterns of the  $\text{CO}_2$  gradient within a leaf are much more complex (Parkhurst, 1994; Aalto and Juurola, 2002). This is, however, not the subject of the present contribution and the assigned boundary condition of  $250\ \text{ppm}\ \text{CO}_2$  fulfils only the function of generating diffusive  $\text{CO}_2$  influx into the model stoma. The program calculates the spatial distribution of gas concentrations within the model space for the steady state. From the concentration patterns, the diffusional fluxes out of and into the stoma are calculated.

According to Vesala (1998) who considered the effects of forced convection (wind) on mass transfer in the leaf boundary layer region, stomatal interference under windy conditions can affect stomatal water vapour diffusion. The effect depends on leaf size and wind velocity (Vesala, 1998). Wind does not significantly influence the diffusion through one single stoma. The present study therefore does not consider the effects of air movements which become essential for the next higher level of leaf gas exchange (i.e. a population of stomata interacting with their specific diffusive properties).

## RESULTS

### Concentration gradients

The expected cup-shaped concentration gradients above the stomatal pore developed for both water vapour and  $\text{CO}_2$ .

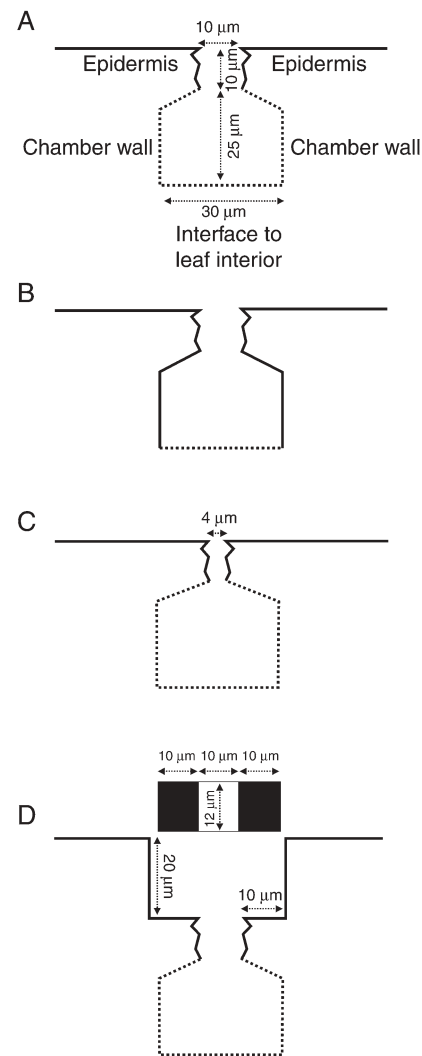


FIG. 2. The different models, depicted in cross-sectional view (cut plane perpendicular to the pore, at the centre of the models). Continuous lines represent non-evaporative sites; dotted lines, sources of water vapour. The bottom of the substomatal chamber represents the interface to the leaf interior. It also represents the sink for  $\text{CO}_2$ . The model dimensions are indicated. The stomatal pore has a length of  $12\ \mu\text{m}$  and a width of  $10\ \mu\text{m}$  for all models, with the exception of the CLOS model (see below). The CHAM and CHAINT models with the larger substomatal chamber are not shown, because the substomatal chamber is increased in the direction perpendicular to the cross-section (see text). They therefore show the same cross-sectional views as BASIC and INTERN. The outlines of both models are shown in Fig. 1. (A) The basic BASIC model; (B) the INTERN model, with the substomatal chamber walls being covered with an internal cuticle; (C) the partially closed CLOS model (pore dimension:  $4 \times 12\ \mu\text{m}$ ); (D) model of a sunken stoma. The stoma is located at the bottom of an antechamber with a depth of  $20\ \mu\text{m}$ . The area of the antechamber amounts to  $12 \times 30\ \mu\text{m}$ . The location of the pore at the bottom of the chamber is depicted as top view above the cross-section with the white rectangle representing the outline of the pore and the black rectangles, the bottom parts of the antechamber.

The contours of water vapour concentration for the model BASIC are plotted in Fig. 3. A steep gradient for water vapour developed within the stomatal channel (see Fig. 4A). In the substomatal chamber, the relative humidity is close to 99 % relative humidity. For  $\text{CO}_2$ , a steep

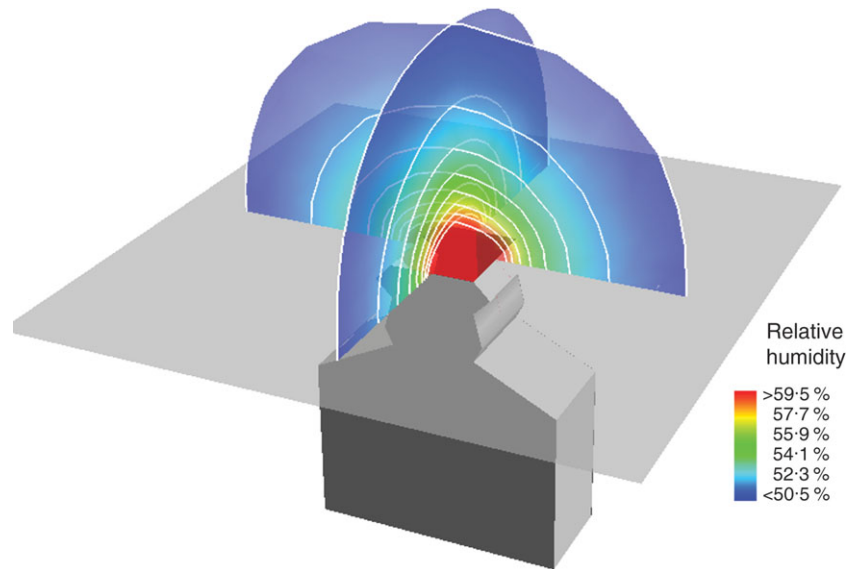


FIG. 3. Spatial pattern of water vapour concentration above the pore of the BASIC model. To allow for visibility of the arrangement of the concentration contours, their cup-shaped arrangement is depicted at two co-ordinate planes intersecting each other at the centre of the stomatal pore.

concentration gradient is also present along the stomatal channel (see Fig. 4B). The  $\text{CO}_2$  gradient in the substomatal chamber is, however, much stronger than the water vapour gradient (see Fig. 4A, B). This is to be expected since  $\text{CO}_2$  has to move from the pore to the chamber floor. The bulging out of the concentration contours at both pore openings of a stoma is included as 'end correction' in equations

describing diffusion through a single stoma, because it increases the effective pore depth (Nobel, 1991). For water vapour, the effect at the internal pore is minimal due to the very low gradient at this site.

In the case of the INTERN model which restricts the water vapour source to the chamber floor, a significant water vapour gradient also developed along the substomatal chamber (Fig. 5). Inside the substomatal chamber of INTERN, significantly lower humidity values are present compared with BASIC. Egorov and Karphushkin (1988) reported leaf internal humidity values of 90–95 %, which correspond roughly with the humidity levels inside the substomatal chamber of INTERN. For the SUNK model, the concentration contours outside of the leaf show a cup-shaped gradient in the cavity above the stomatal pore which gradually straightens out and becomes cup-shaped again above the cavity opening (data not shown).

The gradients of  $\text{H}_2\text{O}$  and  $\text{CO}_2$  are summarized for several models in Fig. 6 by plotting the concentration values from the bottom of the model to its top (maximum

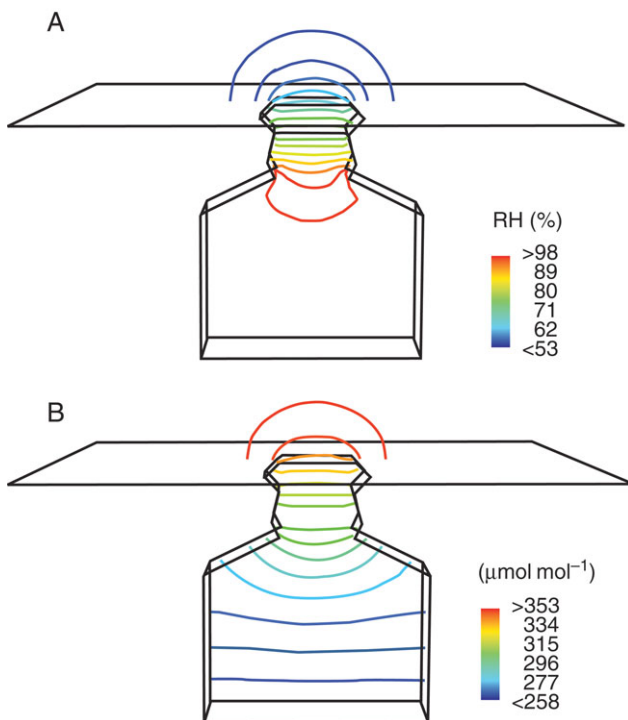


FIG. 4. Concentration gradient inside the model BASIC, plotted as contour lines into a cut plane of the model: (A) contour lines of water vapour, (B) contour lines of  $\text{CO}_2$ .

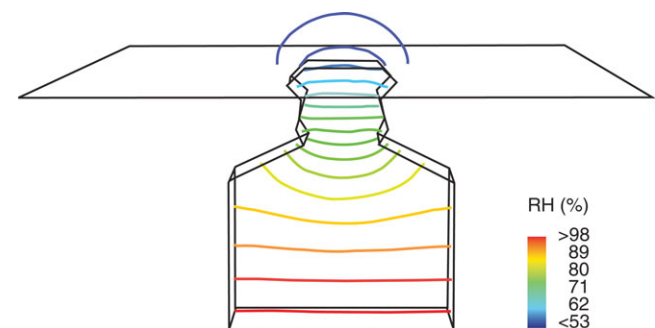


FIG. 5. Concentration gradient of water vapour inside the stomatal model INTERN (model with internal cuticle lining the sides of the substomatal chamber), plotted as contour lines into a cut plane of the model.

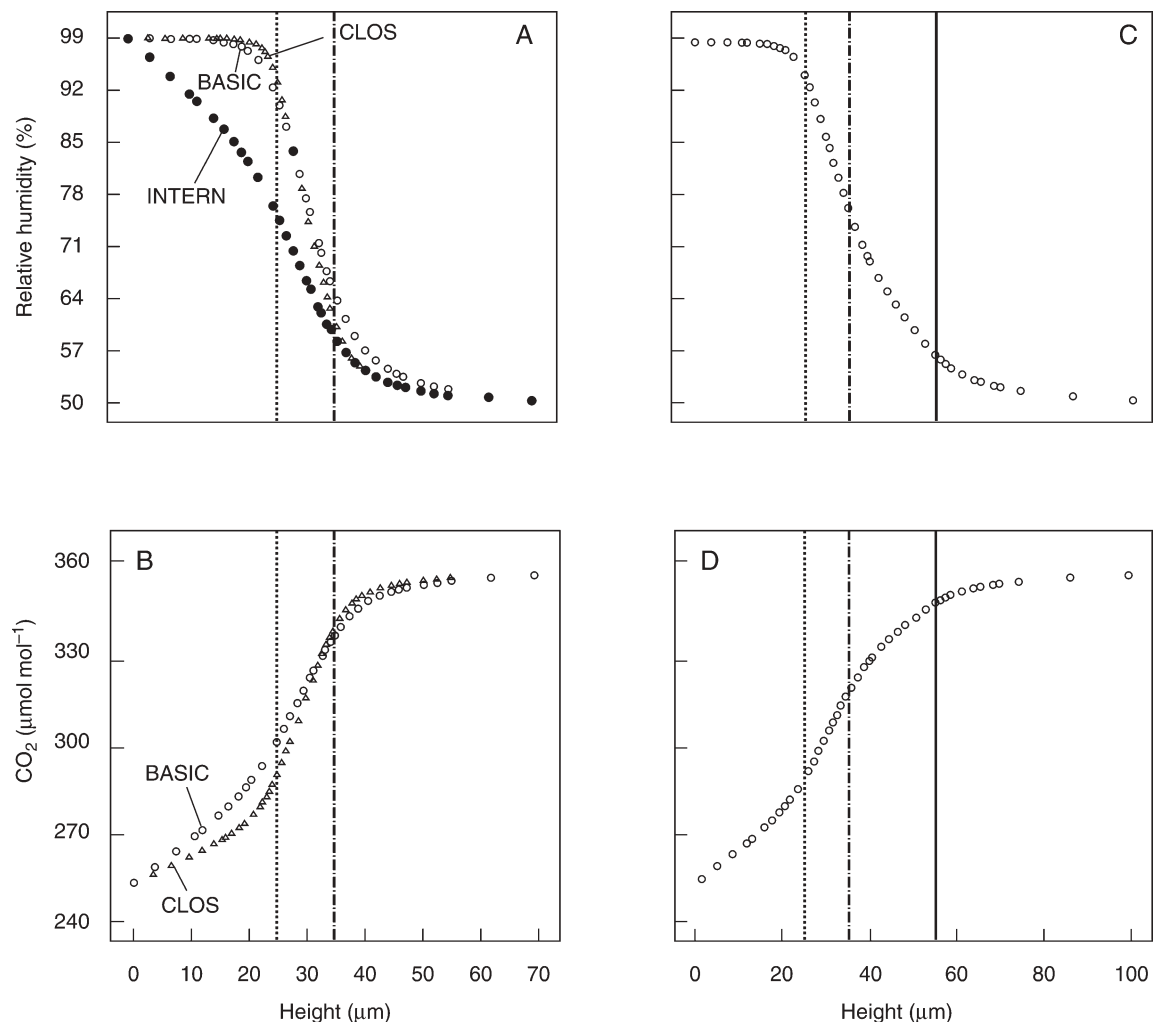


FIG. 6. The gradients of water vapour and  $\text{CO}_2$  depicted for the BASIC, INTERN, CLOS and SUNK models. The concentration values are plotted against the height, from the bottom of each model to its top, at the centre point of the porus. The maximum height amounts to  $70\ \mu\text{m}$  for BASIC, INTERN and CLOS models and to  $100\ \mu\text{m}$  for the SUNK model. (A) Concentration gradient of water vapour for BASIC (open circles), INTERN (filled circles) and CLOS (triangles) models. (B) Concentration gradient of  $\text{CO}_2$  for BASIC (open circles) and CLOS (triangles) models. The INTERN model is not included in this graph since it shows a gradient of  $\text{CO}_2$  which is identical to the BASIC model. (C) Concentration gradient of water vapour for the SUNK model. (D) Concentration gradient of  $\text{CO}_2$  for the SUNK model. Dotted line, internal pore of stomatal chamber; broken line, external pore of stomatal channel; solid line, external orifice of stomatal antechamber.

height =  $70\ \mu\text{m}$  for BASIC, INTERN and CLOS models and  $100\ \mu\text{m}$  for the SUNK model) at the location of the centre point of the pore. The steep concentration gradient for both water vapour and  $\text{CO}_2$  along the stomatal channel is illustrated for all structures. Furthermore, the plots demonstrate the different shapes of the concentration gradients of water vapour and  $\text{CO}_2$  below the stomatal channel in the case of the BASIC, CLOS and SUNK models. The flat water vapour gradient along the substomatal chamber in these models shows that water vapour diffusing into the channel originated preferentially from sites closest to the internal pore. In the INTERN model, which restricts both the water vapour source and the  $\text{CO}_2$  sink to the bottom of the model, a significant water vapour gradient similar to the  $\text{CO}_2$  gradient also developed along the substomatal chamber.

Decreasing of the pore area by partial closure in model CLOS caused a slightly higher gradient above the pore for water vapour and below the pore for  $\text{CO}_2$ . For SUNK, the depression of the stomatal pore resulted in the continuation of the channel gradient along the antechamber which increases the diffusion resistance. This also leads to a higher humidity level directly above the pore.

#### Fluxes of water vapour and $\text{CO}_2$

The flux rates ( $\text{mmol s}^{-1}$  for water vapour, and  $\mu\text{mol s}^{-1}$  for  $\text{CO}_2$ ) per stoma are depicted in Fig. 7. The standard BASIC model attains a water vapour flux of about  $8.5 \cdot 10^{-8}\ \text{mmol s}^{-1}$  and a  $\text{CO}_2$  flux of about  $3 \cdot 10^{-7}\ \mu\text{mol s}^{-1}$ . The elimination of water vapour sources in the immediate vicinity of the pore by the internal cuticle in the INTERN

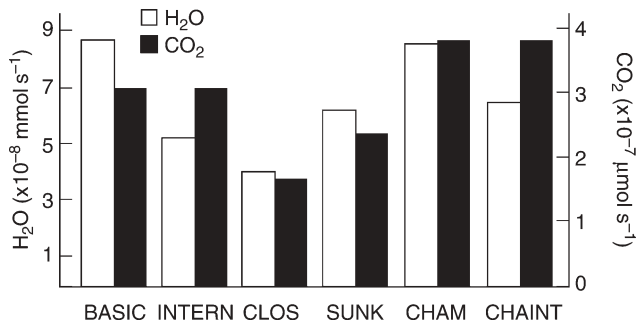


FIG. 7. Diffusive fluxes of the different models, plotted as histogram.

structure leads to a considerable decrease in water vapour flux amounting to  $5 \cdot 10^{-8} \text{ mmol s}^{-1}$  or to about 59 % of the BASIC model. In the case of CO<sub>2</sub>, the flux rates are identical for both BASIC and INTERN since the internal cuticle only affects water vapour. Table 1 provides the flux rates of all model structures as percentage values of the rates attained by the BASIC model (defined as 100 %).

Decreasing the stomatal pore area from  $120 \mu\text{m}^2$  to  $48 \mu\text{m}^2$  in the CLOS model leads to a water vapour flux of  $4 \cdot 10^{-8} \text{ mmol s}^{-1}$  and to a CO<sub>2</sub> flux of  $1.6 \cdot 10^{-7} \mu\text{mol s}^{-1}$ . The fact that the decreases in gas fluxes (amounting to 46 % for water vapour and to 52 % for CO<sub>2</sub> compared with the rates of model BASIC) are less than the decrease in pore area (pore area of SUNK = 40 % of the pore area of the BASIC model) is caused by the circumstance that the pore closure in CLOS is attained by decreasing pore width. This means that the ratio between pore length and pore width and thus pore geometry changes during closing which has an additional effect on conductance (Parlange and Waggoner, 1970). The small difference in the decrease of the flux rates between water vapour and CO<sub>2</sub> is probably due to the different distributions of sinks and sources for the two gases. Since water vapour diffuses towards the internal pore from all sides, whereas CO<sub>2</sub> has to move from the bottom through the whole substomatal chamber, a decrease of the stomatal pore size promotes especially the internal gradient of CO<sub>2</sub>.

For the sunken stoma model SUNK, the additional gradient residing inside the stomatal antechamber decreased the flux rates of both water vapour and CO<sub>2</sub> significantly. The flux rate amounts to about  $6 \cdot 10^{-8} \text{ mmol s}^{-1}$  for water vapour and to  $2 \cdot 10^{-7} \mu\text{mol s}^{-1}$  for CO<sub>2</sub>. The presence of the antechamber resulted therefore in a conductance decrease of about 30 % for both gases. The diffusional flux of water vapour is, however, higher than for the INTERN model (equipped with an internal cuticle).

Enlarging the substomatal chamber in the CHAM model had no substantial influence on water vapour outflux (Fig. 7 and Table 1). CO<sub>2</sub> influx, however, increased by about 24 % (Fig. 1 and Table 1). This is in accordance with the findings of Pickard (1981) who stated that increasing the substomatal chamber size of more than about twice the pore width causes no further significant reduction of transpiration, but should promote CO<sub>2</sub> uptake. The reason for the increase in CO<sub>2</sub> influx is that an enlargement of the substomatal chamber size means an increase of the chamber bottom

size and therefore of the CO<sub>2</sub> sink. The CHAINT model shows the same substomatal chamber size as CHAM, but with an internal cuticle. The diffusional CO<sub>2</sub> influx is identical for both CHAM and CHAINT models (see Fig. 7 and Table 1). The water vapour flux decreases for CHAINT (compared with CHAM) as expected. The transpiration is  $6.4 \cdot 10^{-8} \text{ mmol s}^{-1}$  for CHAINT, which amounts to about 75 % of the transpiration of the CHAM model structure. The reduction in transpiration achieved with an internal cuticle and a larger substomatal chamber (CHAM compared with CHAINT) is therefore lower than with an internal cuticle added to a smaller substomatal chamber (BASIC compared with INTERN) (see Fig. 7 and Table 1).

## DISCUSSION

Sunken stomata are usually interpreted as reducing transpiration. The introduction of an antechamber resulted in a significant reduction in stomatal conductance for the models considered (Fig. 7). There are many types of arrangements which are more complex than the simple antechamber considered here. For example, the stomata in *Nerium oleander* or in *Banksia* are arranged in stomatal crypts filled with hairs (Metcalf and Chalk, 1979; Lösch, 1982). In conifers, the sunken stomata are often additionally capped by a stomatal plug (Napp-Zinn, 1966). It is to be expected that these kinds of crypts offer a larger resistance to diffusion. However, not only transpiration is decreased by stomatal crypts but also CO<sub>2</sub> influx. Sunken stomata therefore also affect assimilation. Feild *et al.* (1998) remark that a '... major conceptual problem with the idea of regulating water loss by a large, fixed resistance in the stomatal porus is that CO<sub>2</sub> uptake would be reduced as well'. Despite the circumstance that both conductance to water vapour and CO<sub>2</sub> are decreased, stomatal antechambers or crypts are probably beneficial for the plant. Feild *et al.* (1998) suggest that the stomatal plugs of *Drimys winteri* decrease wettability of the leaf surface in order to maintain gas exchange and therefore photosynthesis during rain or mist by preventing the formation of a water film covering the stomata. Also *Sequoia sempervirens* growing in fog-inundated regions shows sunken and plugged stomata (Burgess and Dawson, 2004).

Whereas the protection of stomata from the formation of a water film is clearly conceivable as the main function of stomatal crypts in the case of humid and foggy environments, this appears to be less reasonable for arid habitats. Here, sunken stomata or stomata arranged in crypts may be beneficial as an adaptation to drought. Besides decreasing stomatal conductance (which also decreases the rate of the CO<sub>2</sub> influx), it may be speculated that another benefit is the creation of special microclimatic conditions, i.e. higher humidity directly above the stomatal pore. For the simple antechamber arrangement considered in this study, the relative humidity above the pore amounts to about 75 %, whereas it amounts to about 63 % for the non-sunken basic model (Fig. 6). A more elaborate construction, e.g. a stomatal crypt housing more than one stoma and equipped with hairs restricting diffusion further, would achieve a much stronger effect, especially under the conditions of a

thin boundary layer. This microclimate of higher humidity would possibly allow the stomatal pore to be open for much longer time intervals than if the pore were exposed to the lower humidity level at the leaf surface. In fact, Feild *et al.* (1998) observed in the case of stomatal plugs in *Drimys winteri* that these structures are able to prevent stomatal closure, and it was speculated that this phenomenon is possibly due to high levels of humidity at the stomatal pore.

Whereas the depression of a stomatal pore below the leaf surface resulted in a general decrease in the conductance of the stoma, the lining of the substomatal chamber with an internal cuticle mainly affected water vapour (Fig. 7). This is due to the circumstance that water obviously evaporates preferentially in the direct vicinity of the pore, whereas CO<sub>2</sub> drawdown occurs over the whole mesophyll. The phenomenon of intense evaporation close to the stomatal porus is termed as peristomatal transpiration (Lange *et al.*, 1971; Maier-Maercker, 1983). It is suggested that the sensitivity of guard cells to vapour pressure difference in many plant species is correlated with peristomatal transpiration acting as a 'humidity sensor' (Lange *et al.*, 1971; Wullschlegel and Oosterhuis, 1989; Bunce, 1996; Kerstiens, 1996; Maier-Maercker, 1998). Indications of peristomatal transpiration were also found in some former studies: it was demonstrated by both theoretical approaches (Rand, 1977; Tyree and Yianoulis, 1980; Pickard, 1981) and an experimental model (Meidner, 1976) that the largest amount of water vapour leaving a stoma stems from locations near to the stomatal pore if no evaporation barrier is present. The existence of a significant amount of peristomatal transpiration was questioned by Boyer (1985) and by Nonami *et al.* (1990). In both contributions, the important role of an internal cuticle acting as an evaporation barrier suppressing peristomatal transpiration was emphasized.

There are several reports and debates about the existence of an internal cuticle (Scott, 1948; Norris and Bukovac, 1968; Wullschlegel and Oosterhuis, 1989; Nonami *et al.*, 1990; Jeffree, 1996; Pesacreta and Hasenstein, 1999). The main problem is that it is not clear whether this layer (if present) represents a barrier to evaporation. The internal cuticle is reported to be much thinner than the external cuticle (Nonami *et al.*, 1990; Pesacreta and Hasenstein, 1999). This does not, however, necessarily mean that the internal cuticle does not act as a barrier for water vapour. The permeability of a cuticle for water vapour is strongly dependent on its chemical nature (Schreiber *et al.*, 1996). The higher thickness of external cuticles may also be related to mechanical functions or to prevent abrasion (Kerstiens, 1996; Wiedemann and Neinhuis, 1998). In fact, Wullschlegel and Oosterhuis (1989) ascribed the insensitivity of the stomata of *Gossypium hirsutum* to vapour pressure difference to be caused by the presence of an internal cuticle preventing peristomatal transpiration. In the internal cuticles which line the guard cells of *Ulmus glabra*, perforations were found which were interpreted as evaporating sites in the cell walls in order to perceive high vapour pressure difference (Appleby and Davies, 1983). The results of Nonami *et al.* (1990) for *Tradescantia virginiana* indicate that the internal cuticle represents a significant barrier to evaporation.

The substantial effect of the internal cuticle on water vapour diffusion exceeded the decrease in diffusion caused by the stomatal antechamber (Fig. 7). A significant effect of an internal cuticle was also found by Pickard (1981) for a cylindrical model of a substomatal chamber. In this model, the cuticle was located on the underside of the epidermis surrounding the pore which lacked a stomatal channel. An extensive internal cuticle may thus be considered as a suitable device to decrease conductance of water vapour without affecting photosynthesis. The evaporative sites are then forced back into the leaf interior with implications for the pathways of liquid water and water vapour inside a leaf.

In the present study, the internal cuticle also had implications for the effect of substomatal chamber size on transpiration. Enlarging the rectangular substomatal chamber of the present models by increasing the chamber depth did not lead to a significant decrease in transpiration (Fig. 7). In the case of the cylindrical model considered by Pickard (1981), transpiration decreased until the chamber radius amounted to about twice the pore radius. For the smaller rectangular model chamber of the present study, the optimum size was therefore already attained. In a subsequent analysis, Pickard (1982) pointed out that further enlargement of the chamber should promote CO<sub>2</sub> uptake. In the present study, the models with the larger substomatal chambers in fact showed a significantly higher CO<sub>2</sub> influx than the models with the smaller chambers (Fig. 7). The obvious reason for the increase in CO<sub>2</sub> influx is that the cross-sectional area of the diffusion pathway into the leaf interior is larger in the case of the larger substomatal chambers. Contrary to the results of Pickard (1981), however, the model combining a larger substomatal chamber with an internal cuticle showed a higher transpiration than the model with internal cuticle and a smaller substomatal chamber (Fig. 7). This is probably due to the structural differences between the present models and the model of Pickard (1981). In the latter model, the stoma consisted of a circular pore in the ceiling of a cylindrical chamber. The internal cuticle was modelled as a layer covering the internal side of the ceiling around the pore opening. In the present study, the internal cuticle covered the walls of the substomatal chamber. Expanding a substomatal chamber whose walls are covered with an internal cuticle has a promoting effect on both water vapour and on CO<sub>2</sub> diffusion since for both gases the cross-sectional area available for diffusion is increased.

In summary, stomatal structure can have a profound influence on gas conductance, the developing concentration gradients and on the location of the evaporating sites. Precise knowledge concerning concentration gradients in the vicinity of the stomatal pore and within the leaf is significant for analysing stomatal pore width regulation. This is also of high relevance for topics interrelated with water movements inside leaves, such as determination of leaf hydraulic conductance by various methods (Sack *et al.*, 2002), observed correlations between stomatal traits, such as pore area, and hydraulic leaf conductance (Sack and Holbrook, 2006) or distribution of isotopes over the leaf (Barbour and Farquhar, 2003). Numerical simulation

of gas diffusion represents a suitable tool for gaining information about the interrelationship between stomatal structure, gas exchange and evaporation inside a leaf and which is expected to improve our knowledge about the functional role of stomatal features.

## ACKNOWLEDGEMENTS

This work was partially funded by the German ministry of education of research by a grant to A.R.-N (No. 0311973). I thank Wilfried Konrad for helpful and stimulating discussions and James Nebelsick for critically reading the English manuscript.

## LITERATURE CITED

- Aalto T, Juurola E. 2002. A three-dimensional model of CO<sub>2</sub> transport in airspaces and mesophyll cells of a silver birch leaf. *Plant, Cell and Environment* **25**: 1399–1409.
- Appleby RF, Davies WJ. 1983. A possible evaporation site in the guard cell wall and the influence of leaf structure on the humidity response by stomata of woody plants. *Oecologia* **56**: 30–40.
- Ball JT, Woodrow IE, Berry JA. 1987. A model predicting stomatal conductance and its contribution to the control of photosynthesis under different environmental conditions. In: Biggins I, ed. *Progress in photosynthesis research*. Dordrecht: Martinus Nijhoff Publishers, 221–224.
- Barbour MM, Farquhar GD. 2003. Do pathways of water movement and leaf anatomical dimensions allow development of gradients in H<sub>2</sub>O between veins and the sites of evaporation within leaves? *Plant, Cell and Environment* **27**: 107–121.
- Boyer JS. 1985. Water transport. *Annual Review of Plant Physiology* **36**: 473–516.
- Brodribb T, Hill RS. 1997. Imbricacy and stomatal wax plugs reduce maximum leaf conductance in southern hemisphere conifers. *Australian Journal of Botany* **45**: 657–668.
- Brown HT, Escombe F. 1900. Static diffusion of gases and liquids in relation to the assimilation of carbon and translocation in plants. *Philosophical Transactions of the Royal Society of London Series B* **193**: 223–291.
- Buckley TN, Mott KA, Farquhar GD. 2003. A hydromechanical and biochemical model of stomatal conductance. *Plant, Cell and Environment* **26**: 1767–1785.
- Bunce JA. 1996. Does transpiration control stomatal responses to water vapour pressure deficit? *Plant, Cell and Environment* **19**: 131–135.
- Burgess SSO, Dawson TE. 2004. The contribution of fog to the water relations of *Sequoia sempervirens* (D. Don): foliar uptake and prevention of dehydration. *Plant, Cell and Environment* **27**: 1023–1034.
- Collatz GJ, Ball JT, Griwet C, Berry JA. 1991. Physiological and environmental regulation of stomatal conductance, photosynthesis, and transpiration: a model that includes a laminar boundary layer. *Agricultural and Forest Meteorology* **54**: 107–136.
- Egorov VP, Karpushkin LT. 1988. Determination of air humidity over evaporating surface inside a leaf by a compensation method. *Photosynthetica* **22**: 394–404.
- Farquhar GD, Raschke K. 1978. On the resistance to transpiration of the sites of evaporation within the leaf. *Plant Physiology* **61**: 1000–1005.
- Farquhar GD, Wong SC. 1984. An empirical model of stomatal conductance. *Australian Journal of Plant Physiology* **11**: 191–210.
- Feild TS, Zwieniecki MA, Donoghue MJ, Holbrook NM. 1998. Stomatal plugs of *Drimys winteri* (Winteraceae) protect leaves from mist but not drought. *Proceedings of the National Academy of Sciences of the USA* **95**: 14256–14259.
- Franks PJ, Farquhar GD. 1999. A relationship between humidity response, growth form and photosynthetic operating point in C3 plants. *Plant, Cell and Environment* **22**: 1337–1349.
- Jeffree CE. 1996. Structure and ontogeny of plant cuticles. In: Kerstiens G, ed. *Plant cuticles – an integrated functional approach*. Oxford: BIOS Scientific Publishers.
- Kerstiens G. 1996. Signaling across the divide: a wider perspective of cuticular structure–function relationships. *Trends in Plant Science* **1**: 125–129.
- Lange OL, Lösch R, Schulze E-D, Kappen L. 1971. Responses of stomata to changes in humidity. *Planta* **100**: 76–86.
- Larcher W. 2003. *Physiological plant ecology*, 4th edn. Cambridge: Cambridge University Press.
- Leuning R. 1990. Modeling stomatal behaviour and photosynthesis of *Eucalyptus grandis*. *Australian Journal of Plant Physiology* **17**: 159–175.
- Lösch R, Tenhunen JD, Pereira JS, Lange OL. 1982. Diurnal courses of stomatal resistance and transpiration of wild and cultivated Mediterranean perennials at the end of the summer dry season in Portugal. *Flora* **172**: 138–160.
- Lushnikov AA, Vesala R, Kulmala L, Hari P. 1994. A semiphenological model for stomatal gas transport. *Journal of Theoretical Biology* **171**: 291–301.
- Maier-Maercker U. 1983. The role of peristomatal transpiration in the mechanism of stomatal movement. *Plant, Cell and Environment* **6**: 369–380.
- Maier-Maercker U. 1998. Dynamics of change in stomatal response and water status of *Picea abies* during a persistent drought period: a contribution to the traditional view of plant water relations. *Tree Physiology* **18**: 211–222.
- Meidner H. 1976. Water vapour loss from a physical model of a substomatal cavity. *Journal of Experimental Botany* **27**: 691–694.
- Metcalfe CR, Chalk L. 1979. *Anatomy of the dicotyledons*. Vol. I. *Systematic anatomy of the leaf and stem*, 2nd edn. Oxford: Clarendon Press.
- Napp-Zinn K. 1966. *Anatomie des Blattes*. II. *Blattanatomie der Gymnospermen*. Berlin: Gebrüder Bornträger.
- Napp-Zinn K. 1973. *Anatomie des Blattes*. II. *Blattanatomie der Angiospermen*. Berlin: Gebrüder Bornträger.
- Nobel PS. 1991. *Physicochemical and environmental plant physiology*. San Diego, CA: Academic Press.
- Nonami H, Schulze E-D, Ziegler H. 1990. Mechanisms of stomatal movement in response to air humidity, irradiance and xylem water potential. *Planta* **183**: 57–64.
- Norris RF, Bukovac MJ. 1968. Structure of the pear leaf cuticle with special reference to cuticular penetration. *American Journal of Botany* **55**: 975–983.
- Parkhurst DF. 1994. Diffusion of CO<sub>2</sub> and other gases inside leaves. *New Phytologist* **126**: 449–479.
- Parlange J-Y, Waggoner PE. 1970. Stomatal dimensions and resistance to diffusion. *Plant Physiology* **46**: 337–342.
- Pesacreta TC, Hasenstein KH. 1999. The internal cuticle of *Cirsium horridulum* (Asteraceae) leaves. *American Journal of Botany* **86**: 923–928.
- Pickard W. 1981. How does the shape of the substomatal chamber affect transpirational water loss? *Mathematical Biosciences* **56**: 111–127.
- Pickard W. 1982. Why is the substomatal chamber as large as it is? *Plant Physiology* **69**: 971–974.
- Rand RH. 1977. Gaseous diffusion in the leaf interior. *Transactions of the American Society of Agricultural Engineers* **20**: 701–704.
- Sack L, Holbrook NM. 2006. Leaf hydraulics. *Annual Review of Plant Biology* **57**: 361–381.
- Sack L, Melcher PJ, Zwieniecki MA, Holbrook NM. 2002. The ‘hydrology’ of leaves: co-ordination of structure and function in temperate woody species. *Plant, Cell and Environment* **26**: 1343–1356.
- Schreiber L, Kirsch T, Riederer M. 1996. Diffusion through cuticles: principles and models. In: Kerstiens G, ed. *Plant cuticles – an integrated functional approach*. Oxford: BIOS Scientific Publishers.
- Scott FM. 1948. Internal suberization of plant tissues. *Science* **108**: 645–655.
- Tyree MT, Yianoulis P. 1980. The site of water evaporation from substomatal cavities, liquid path resistances and hydroactive stomatal closure. *Annals of Botany* **46**: 175–193.
- Van Gardingen PR, Jeffree CE, Grace J. 1989. Variation in stomatal aperture in leaves of *Avena fatua* L. observed by low-temperature

- scanning electron microscopy. *Plant, Cell and Environment* **12**: 887–898.
- Vesala T. 1998.** On the concept of leaf boundary layer resistance for forced convection. *Journal of Theoretical Biology* **194**: 91–100.
- Vesala T, Hämeri K, Ahonen T, Kulmala M, Hari P, Pohja T, et al. 1995.** Experimental and numerical analysis of stomatal absorption of sulphur dioxide and transpiration by pine needles. *Atmospheric Environment* **29**: 825–836.
- Vesala T, Ahonen T, Hari P, Krissinel E, Shokirev N. 1996.** Analysis of stomatal CO<sub>2</sub> uptake by a three-dimensional cylindrically symmetric model. *New Phytologist* **132**: 235–245.
- Wiedemann P, Neinhuis C. 1998.** Biomechanics of isolated plant cuticles. *Botanica Acta* **111**: 28–34.
- Wullschleger SD, Oosterhuis DM. 1989.** The occurrence of an internal cuticle in cotton (*Gossypium hirsutum* L.) leaf stomates. *Environmental and Experimental Botany* **29**: 229–235.
- Yianoulis P, Tyree MT. 1984.** A model to investigate the effect of evaporative cooling on the pattern of evaporation in sub-stomatal cavities. *Annals of Botany* **53**: 189–206.
- Zienkiewicz OL, Taylor RL. 1989.** *The Finite Element Method*, 4th edn. London: McGraw-Hill.